Composites Science and Technology 181 (2019) 107703

Contents lists available at ScienceDirect

Composites Science and Technology

journal homepage: www.elsevier.com/locate/compscitech

The effect of temperature and water immersion on the interlaminar shear fatigue of glass fiber epoxy composites using the I-beam method

Abedin I. Gagani*, Anna B. Monsås, Andrey E. Krauklis, Andreas T. Echtermeyer

Department of Mechanical and Industrial Engineering, Norwegian University of Science and Technology (NTNU), Trondheim, Norway

ARTICLE INFO

Keywords:
Polymer-matrix composites (PMCs)
Durability
Environmental degradation
Fatigue
Hygrothermal effect

ABSTRACT

This work investigates the combined effect of water immersion and temperature on the interlaminar shear static and fatigue strength of glass fiber epoxy composites. Interlaminar shear tests were performed on I-beam shaped samples which enable faster fluid saturation at 20, 40 and 60 °C, both in air and in immersion. Analysis of fatigue parameters and optical micrography enabled understanding the phenomena that govern the static and fatigue degradation for each case. The dry properties are dominated by the matrix resistance at room temperature and by fiber/matrix interface strength for higher temperature. The immersed properties are dominated by the fiber/matrix interface degradation. An analytical model based on Arrhenius theory is presented for building a fatigue mastercurve that accounts for both temperature and water immersion. The effect of water immersion is modelled by accounting for the change of glass transition temperature of the material. The results show that the mastercurve describes well the conditions tested, provided that the material remains below its glass transition temperature.

1. Introduction

In the recent years interest for composite material in the offshore industry has grown due to their corrosion resistance and lightweight [1]. Many projects have provided in field experience using composites offshore [2] verifying their excellent resistance. One of the main challenges encountered in these projects has been the great number of tests required to certify these composite structures, which leads to high costs. To reliably ensure resistance for very long operational lives, the mechanical properties and performance of the material need to be tested in various environmental conditions, representative of the ones that the structure is expected to encounter in the application (Fluid immersion, high/low temperatures, gas permeation and chemical attack). If the same structure is later employed in another oilfield the environmental conditions can change with respect to the ones considered during the testing and certification of the structure, requiring additional testing and verifications.

The high costs related to testing and certification and the difficulty in extrapolation of the results for different test conditions are probably the major hinder for an increase in the use of composites offshore. It is therefore beneficial to reduce the number of tests to perform at different temperatures and environments.

In this work a glass fiber reinforced epoxy was tested statically and cyclically under different conditions: dry and saturated with water, in different temperatures (20 °C, 40 °C and 60 °C). The failure mechanisms were analysed for the different conditions and an Arrhenius master curve was proposed, which models both temperature and water saturation.

The failure mode tested and analysed in this work is interlaminar shear fatigue. This has been chosen since it is one of the failure modes most effected by environmental degradation, as it is dominated by the properties of the matrix and the fiber/matrix interface. In fact, in real applications composite structured are always connected to other materials, typically metallic. This connection causes high interlaminar stresses, since fibers do not run from the composite to the metal, which often can lead to failure. It is therefore very important to assess the variation of interlaminar durability.

Many standard methods are available for through-the-thickness shear testing of composites [3], but it is hard to find a test method that allows quick saturation of the sample, due to the high thickness of most test samples. In fact, Fickian diffusion theory suggests that the time needed to reach saturation is proportional to the square of the thickness of the laminate. Thin laminates would therefore be beneficial to adopt.

This article concentrates on measuring shear based on a variation of the Short Beam Shear (SBS) test [4]. If a SBS test is done on very thin samples the test is difficult or impossible to carry out, because the

* Corresponding author.
E-mail address: abedin.gagani@ntnu.no (A.I. Gagani).

https://doi.org/10.1016/j.compscitech.2019.107703
Received 22 December 2018; Received in revised form 16 June 2019; Accepted 25 June 2019
Available online 27 June 2019

sample bends too much if the samples are tested in a horizontal position and roller indentation from the fixture becomes a problem if the samples are tested vertically. A good compromise between accelerating saturation and avoiding indentation effects has been found by adopting I-beam shaped bending samples, which combine a thin central web and wider top and bottom flanges. These have the advantage of requiring only few weeks to reach saturation (the web is 2 mm thick) and yet reduce roller indentation due to the presence of top and bottom flanges thanks to the adoption of a four-point bending configuration, similarly to the standard for interlaminar shear testing of sandwich structures. Milling of the I-beam samples from a laminate is a complex operation, but the reduction of sample thickness has drastic effects on the saturation time of the material, since this is a quadratic function of the thickness. A thickness reduction by half, for example, results in a four times shorter saturation times, which can spare several months of testing. The I-beam test method has been presented and discussed in Refs. [5,6], where it was shown that the static behavior of the samples could be well predicted from the nonlinear behavior of the matrix, while linear elastic theory leads to an overestimation of the interlaminar shear strength of the material. The test setup and sample geometry are shown in Fig. 1 (a, b).

Environmental effects on interlaminar shear strength of composites have been studied experimentally since early works of Springer, reporting a decrease of performance due to both moisture and higher temperature [7,8]. Similar effects were also found by Browning, Husman and Whitney [9]. This effect is very likely to be caused by the degradation of the fiber/matrix (F/M) interface, as suggested by the single-fiber-fragmentation-test (SFFT) performed by Ramirez et al. [10]. The fiber/matrix interface plays an important role on the thermal and hygroscopic properties of the composites. Mallarino et al. [11] and later Joliff et al. [12,13] have shown that the interphase has a much lower glass transition temperature compared to the matrix, due to localized incomplete curing or plasticizing effects from fiber treatment. This fiber/matrix interphase, together with the matrix plays an important role in the interlaminar shear behaviour of the material [14].

The damage mechanisms of interlaminar shear failure were studied in recent works from Rocha et al. [15,16] and from the authors [5]. In dry samples the failure was a creep dominated effect, as discussed by Petermann and Schulte [17], while for conditioned samples the fatigue behaviour was governed by the growth of fiber/matrix interface debondings [5,16]. The effect of temperature on the fatigue of dry and conditioned samples was modelled analytically by Mortazavian and Fatemi [18], which used an Arrhenius approach, as suggested by Nakada and Myiano [19].

In this work the failure mechanism of composites dry and immersed in water is studied at different temperatures. The micromechanical mechanisms of damage are analysed and a mastercurve based on Arrhenius theory is proposed for the description of the effect of both temperature and water saturation.

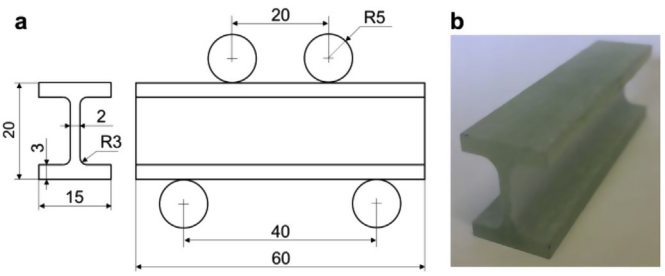

Fig. 1. (a) Set up geometry and dimensions of tested I-beam samples and (b) I-beam specimen.

2. Material and methods

2.1. Materials

A glass fiber/epoxy composite laminate has been manufactured using vaacum assisted resin transfer molding (VARTM). The matrix was Hexion Epikote™ Resin RIMR135 mixed with Epikure™ Curing Agent MGS RIMH137 with a mixing ratio of 100:30 by weight. The fibers were HiPer-tex™ UD glass fibers from 3B. Curing was performed at room temperature for 24 h and post-curing in a ventilated oven at 80 °C for 16 h.

The volume fraction of the laminate was obtained by matrix burnoff test, resulting in 54.0%.

A set of samples was immersed in 60 °C distilled water until saturation occurred, according to ASTM D5229 Standard.

The laminate obtained was cut into rectangular bars using a diamond coated saw, and milled to the I-beam geometry, shown in Fig. 1. The individual samples were then cut to 60 mm length using a water-cooled diamond coated saw. In order to reduce potential stress concentrations, the edges of the samples were ground up to a 4000 grit and polished with a 3 μm polishing disc. In Ref. [5] the fatigue performance of the I-beam samples was compared with standard test results from the literature yielding a good agreement. This suggested that the grinding and polishing procedure reported here enables a good surface roughness and avoids surface crack initiation.

Prior to hygrothermal conditioning and testing all the samples were dried in an oven at 50 °C for 72 h. A set of samples destined to immersed testing was immersed in distilled water in a thermally regulated chamber at 60 ± 1 °C until saturation occurred, according to ASTM D5229 Standard [20]. The samples immersed in distilled water were weighed using a Mettler Toledo AG204 DeltaRange scale, having a sensibility of ± 0.1 mg.

Dynamic thermal mechanical characterization of the material was performed on dry and conditioned tensile samples using a Netzsch-Gabo Eplexor 150 DMTA machine equipped with a 150 N load cell and a thermal chamber, resulting in glass transition temperature, T_g = 87.1 °C for dry samples and T_g = 49.0 °C for conditioned samples [5,6].

2.2. Interlaminar static and fatigue testing

Four-point bending testing was performed on the I-beam short beam shear configuration shown in Fig. 1, using a Schenk tensile machine with a 12,5 kN loadcell and a customized chamber for the immersed tests and a MTS Landmark machine with a 50 kN loadcell and a MTS651 environmental chamber for high temperature dry tests. The tests were performed in load control, with a ratio R = 0.1 and a frequency of 4 Hz, in order to reduce the effect of heat generated by loading. For samples that reached 2 000 000 cycles, the test was stopped and the result was defined as a run-out. The setup used for the dry and immersed test is shown in Fig. 2(a–b). A polycarbonate (PC) antibuckling device was used in order to avoid buckling of the sample's central web, as shown in Fig. 2(a–b) and discussed in Refs. [5,6]. The antibuckling device was designed to avoid initiation of buckling in the web of the sample, to obtain a valid shear failure. A very small clamping force was used, to avoid constrain stresses in the web of the sample. Failure was defined when the samples reached a limit deflection equal to the static deflection at failure for that test environment (dry or conditioned). In Fig. 2 (c) are reported other possible definitions of failure for a SBS test, like the knee of the deflection curve or the limit of the set-up, when further deflection would damage the set-up. The static deflection at failure was chosen since it is the most reproducible criterion. It was verified that the choice of the failure criterion has little influence for the material studied here. A comparison was performed on the conditioned samples tested at 40 °C, by comparing the number of cycles to ultimate static deflection (1.87 mm) with the number of cycles

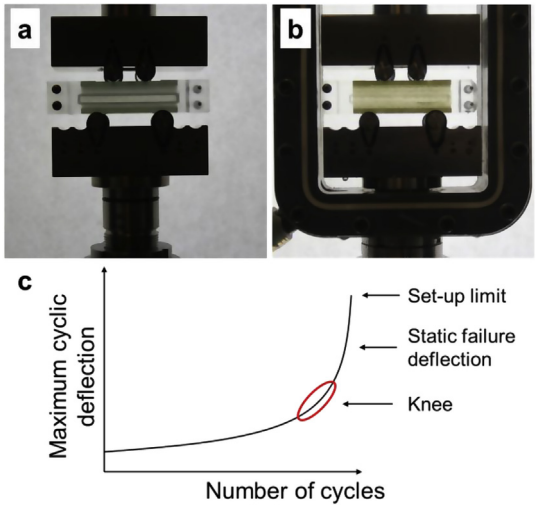

Fig. 2. Test set up for (a) immersed and (b) tests. (c) Schematic evolution of maximum cyclic deflection.

to the highest allowable deflection of the set-up (3.00 mm). The difference in fatigue life was between 1.8 and 6.2% for long and short fatigue lives respectively. When dealing with different materials it is recommended to verify the validity of this assumption.

3. Results

3.1. Fluid saturation

The results of the mass gain measurement are shown in Fig. 3. Saturation was defined according to the standard [20], when the difference between two consecutive measurements was less than ± 0.02%.

It can be noticed that saturation occurs at 0.72% mass increase. This value is a bit lower than the one measured in Ref. [21] on the same material. The difference can be attributed to the different volume fraction of the laminate compared to the one studied in Ref. [21]: 59.5%.

3.2. Static results

The static load deflection curves are shown in Fig. 4.

It can be noticed that there is a progressive decrease in strength for the dry and conditioned samples with higher temperatures. The tangential elastic modulus was estimated from the slope of the linear part of the load-deflection curve according to Timoshenko's beam theory [22]. The results are summarized in Table 1 and are shown in Fig. 5.

The tangential elastic modulus obtained from the crosshead displacement is computed in the initial linear part of the load-deflection curve, below 50% ultimate load. This was done in order to reduce the incidence of roller indentation on the results.

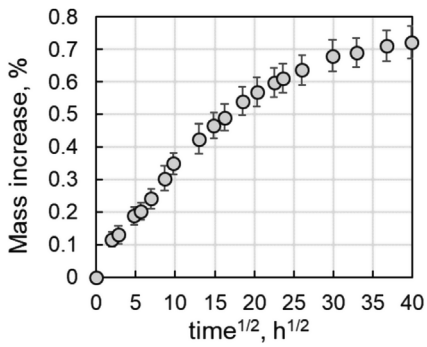

Fig. 3. Mass increase of the tested samples.

It can be noticed that the ultimate load is very sensitive to the increase in temperature in both the dry and conditioned specimens. The tangent elastic modulus, on the other hand, is almost not influenced by the temperature for the dry case and slightly influenced by the temperature for the conditioned case. This difference is attributed to the fact that the conditioned samples are tested closely below and above the glass transition temperature, which is 49 °C for saturated samples. When reaching the glass transition temperature, the material starts to transform into a rubbery state, which explains the strong decrease in elastic properties, Fig. 5.

From the static curves of the I-beams, Fig. 4, it is possible to obtain the degraded properties of the matrix, using the FE method proposed in Ref. [6], where the I-beam is modelled using a laminated approach, where the matrix degradation is considered using an elasto-plastic formulation.

Optical micrographs were performed on statically tested samples and are shown in Fig. 6.

From the optical micrographs on statically tested samples it can be noticed that failure occurs in the central web of the I-beams in form of intra-ply cracks. The only exception is the dry sample tested at 20 °C, which showed in inter-laminar crack. A similar trend will be shown in the next paragraph for the cyclically tested samples.

3.3. Fatigue results

The SN curves are shown in Fig. 7 where the maximum load is plotted along with the number of cycles to failure. The R ratio was 0.1. The results were interpolated using the Basquin relation [23]:

$$L = L_0 N^{-1/k} \quad (1)$$

where L is the maximum load, L_0 is the pre-exponential load coefficient, N is the number of cycles and k is the slope. The interpolation parameters are reported in Table 2.

For the dry samples, it is possible to notice a difference between the slope of the SN curve at 20 °C and the SN curves at 40 °C and 60 °C. The slopes at 40 °C and 60 °C seem flatter than the slopes of the curve at 20 °C. This difference can be attributed to a change in fatigue failure mechanism. It will be shown in the discussion that the dry sample's damage at 20 °C is governed by the creep in the matrix, while at higher temperatures (40 and 60 °C) the mechanism is governed by creep in the fiber/matrix interphase.

For the conditioned SN curves, it is possible to observe a similar slope for the samples tested at 20 °C and 40 °C, while the samples tested at 60 °C showed a different slope. The latter is attributed to the regime above the glass transition temperature.

From Table 2 it is possible to identify three categories of slopes of SN curves: the slopes of the dry specimens (0.0538, 0.0355 and 0.042), the slopes of conditioned specimens tested at 20 °C and 40 °C (0.0709 and 0.0734) and the slopes of conditioned specimens tested at 60 °C (0.1065). These observations suggest a potential change in failure mechanisms, which is analysed in more detail in the following sections.

The hysteresis loops shown in Fig. 8 provide a first qualitative analysis of the samples mechanical degradation during the test. It is possible to notice that for the dry samples, Fig. 8 (a, b and c), the curves shift toward greater deflections during the fatigue test. This effect is enhanced by the increase in temperature. The change in slope of the hysteresis loops is quite small during the tests, while a slight increase of the area of the hysteresis curves is visible with increasing temperatures. The conditioned samples tested in immersion at 20 and 40 °C, Fig. 8 (d, e), show also a shift of the hysteresis loops toward greater deflections during the fatigue test, but in this case also a strong decrease in slope and increase in area of the hysteresis loops is visible.

For the conditioned samples tested above their T_g, Fig. 8 (f), the hysteresis loops show a very particular behaviour, they shift toward

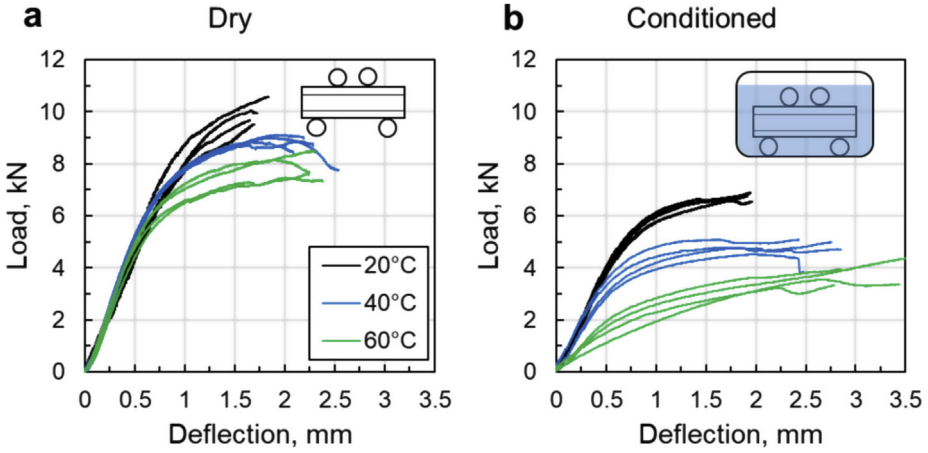

Fig. 4. Static results for (a) dry and (b) conditioned samples, tested at 20 °C, 40 °C and 60 °C.

Table 1
Ultimate load and elastic tangential modulus for different environmental conditions.

State	Ultimate load (kN)	Tangent elastic modulus (MPa)
Dry – 20 °C	9.95 ± 0.46	2930 ± 176
Dry – 40 °C	8.75 ± 0.07	3090 ± 109
Dry – 60 °C	7.33 ± 0.51	2880 ± 172
Conditioned – 20 °C	6.57 ± 0.04	2090 ± 2
Conditioned – 40 °C	4.79 ± 0.23	1800 ± 265
Conditioned – 60 °C	3.45 ± 0.17	870 ± 236

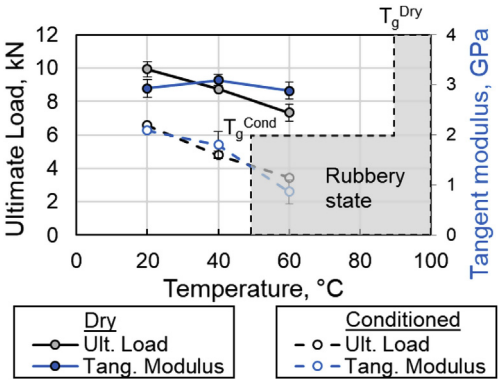

Fig. 5. Ultimate load and tangent modulus from static tests, the glass transition temperature and beginning of glassy state for the material are highlighted.

greater deflections very quickly and don't show a strong change of slope or area. It is believed that this effect is attributed to the rubbery state reached by the material.

To analyse the observed failure mechanism, it is useful to isolate the contribution of creep and damage growth during the fatigue lives. In Figs. 9, 10 and 12 the dynamic secant tangent modulus, hysteresis dissipated energy and minimum/maximum cyclic deflection are shown and the results are analysed.

The analysis presented here is based on samples tested between 5 10^4 and 10^5 cycles to failure, which were loaded cyclically below 60% of their ultimate load. This level of loading was chosen to reduce the influence of roller indentation on the analysis to a negligible level.

The dynamic secant modulus of the dry samples shows a typical three stage behaviour for every test temperature: I – initial drop of modulus in the first 20% of the fatigue life, II – steady reduced decrease in modulus and III – final degradation prior to failure after 80% of the fatigue life, Fig. 9. For the conditioned samples the behaviour is different. At 20 °C and 40 °C the modulus decreases steadily during the entire fatigue life; this effect is more marked at 40 °C. At 60 °C the modulus is constant during the entire life, but much smaller than in the dry case. This effect is attributed to the change in properties occurring above the glass transition temperature: the sample degrades almost instantly from the beginning of the fatigue test. It is important to remark that the secant modulus describes only the change of slope of the hysteresis cycles, whereas the tangent modulus would be influenced by the "rigid" shift of the hysteresis loops. This characteristic makes the secant modulus useful for the description of damage mechanisms, as it is not influenced by creep, which causes a "rigid" shift of the hysteresis loops.

In Fig. 10 are shown the maximum and minimum cyclic deflection for each cycle. The minimum cyclic deflection is an indication of non-reversible deformation occurring, typically associated with creep or damage development. The deviation between minimum and maximum cyclic deflection gives information about the elastic degradation of the material, as the fatigue test is run in load control. For the dry state it can be noticed that in the range of temperatures studied the material has a similar behaviour, an initial state with increase in cyclic deflection up to 20% of the fatigue life, a small increase in deflection between 20 and 80% of the fatigue life and an increase of the deflection in the last 20%. The last stage is also the one where the difference between minimum and maximum cyclic deflection increases, suggesting a degradation affects the elastic modulus. For the conditioned material the 20 °C state shows a behaviour similar to the dry one, the 40 °C shows only phase I and III, initial and final increase in deflection. For the samples tested at 60 °C the behaviour observed is consistent with a rubbery behaviour.

All samples shown in Fig. 11 have been cyclically tested to failure, which occurred between 10^4 and 10^5 cycles. The dry and conditioned samples tested at 20 °C failed at 29416 and 29229 cycles respectively at a load of 6.24 and 3.6 kN. The dry and conditioned samples tested at 40 °C failed at 42355 and 63568 cycles respectively at a load of 5.69 and 2.63 kN. The dry and conditioned samples tested at 60 °C failed at 20625 and 22496 cycles respectively at a load of 4.46 and 1.56 kN.

Another parameter that provides information about the damage mechanism is the cyclic hysteresis dissipated energy, Fig. 12, defined as the area inside each hysteresis loop. For the dry samples it is possible to notice that the increase of hysteresis dissipated energy is very small during most of the fatigue life and presents an increase in the final 80% of the fatigue life. For the conditioned samples an increase of the hysteresis dissipated energy occurs during the entire fatigue life. This effect is stronger with the increase in temperature, suggesting that a mechanical degradation is occurring. For the conditioned samples tested at 60 °C the hysteresis dissipated energy is constant and very small during the entire fatigue life, suggesting that a purely rubbery behaviour is developing.

Microscopy analysis, Fig. 13, show that dry samples tested at 20 °C

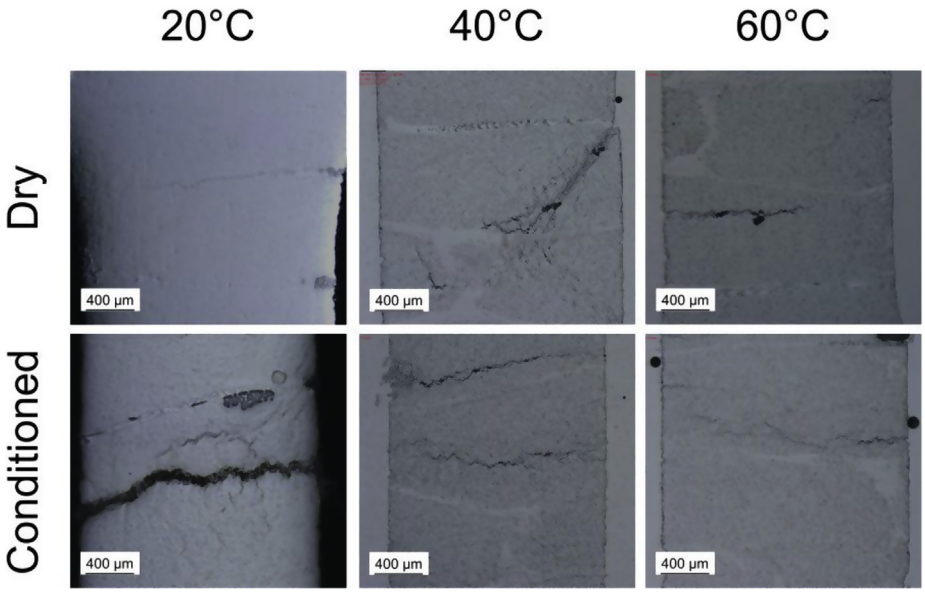

Fig. 6. Optical micrograph for dry and conditioned samples statically tested at 20, 40 and 60 °C.

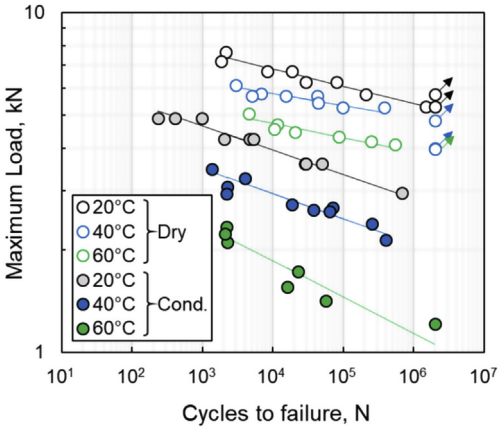

Fig. 7. Fatigue SN curves for dry samples tested in air and conditioned samples tested in immersion.

Table 2
Parameters using for interpolating the SN curves, according to Eq. (2).

Environmental condition	L_0 (kN)	1/k (−)
Dry – 20 °C	11.85 ± 0.33	0.0538
Dry – 40 °C	8.01 ± 0.23	0.0355
Dry – 60 °C	6.96 ± 0.20	0.0420
Conditioned – 20 °C	7.59 ± 0.25	0.0709
Conditioned – 40 °C	5.76 ± 0.43	0.0734
Conditioned – 60 °C	4.96 ± 0.51	0.1065

failed due to inter-ply cracks, when increasing the temperature, the crack developed in the intra-ply. For conditioned samples, the crack developed in the intra-ply for both room temperature and higher temperature.

Microscope analysis of untested samples, Fig. 14, showed the presence of fiber/matrix debonding prior to testing. This effect is consistent with recent works [5,16].

4. Discussion

4.1. Static behaviour

The static results reported in Figs. 4 and 5 show that the temperature has a small influence on the elastic tangential modulus of the dry material, similarly to the results observed by Manalo et. for dry material [24]. On the other hand, for the conditioned material an increase in temperature caused a decrease of the elastic tangential modulus. This difference is attributed to the fact that the dry material is tested well below its glass transition temperature (87.1 °C), while the conditioned samples are tested close to it (49.0 °C).

The stronger influence of the temperature on the interlaminar shear strength, Figs. 4 and 5, is consistent with the results reported by Davies and Arhant, [25]. This effect could be attributed to the influence of the fiber/matrix interphase in the interlaminar failure of composites. Mallarino et al. [11] and Joliff et al. [12,13] have shown that the fiber/matrix interface has locally a glass transition temperature much lower than the one of the bulk matrix, this can explain the sensitivity of the interlaminar shear strength to the temperature.

4.2. Fatigue behaviour

The different slopes in the SN curves, shown in Fig. 6 and reported in Table 2 are caused by changes of microscale mechanisms that cause failure. For the dry samples tested at 20 °C, failure was shown to initiate as cracks in the inter-ply [5], while at higher temperatures, 40 and 60 °C, the microscopy analysis showed intra-ply cracks, Fig. 12. Although the temperature has an influence on the location of failure for the dry samples, from inter-ply to intra-ply, the analysis of dynamic secant modulus, Fig. 9, minimum/maximum cyclic deflection, Fig. 10, and hysteresis dissipated energy, Fig. 12, show a similar behaviour in all cases. For the dry samples, failure seems to be a creep governed effect, however the temperature has an influence on the location where creep failure occurs. At 20 °C the failure occurs in the inter-ply, a resin rich area, while at 40 °C and 60 °C the failure occurs inside the ply, in the intra-ply. The reason for this difference is believed to be the locally lower glass transition of the fiber/matrix interface, as shown by Mallarino et al. [11] and Joliff et al. [12,13].

For the conditioned SN curves at 20 °C and 40 °C the slopes were similar, suggesting that both cases lead to a similar failure mechanism. In fact, in Ref. [5] it was shown that fiber/matrix debondings were

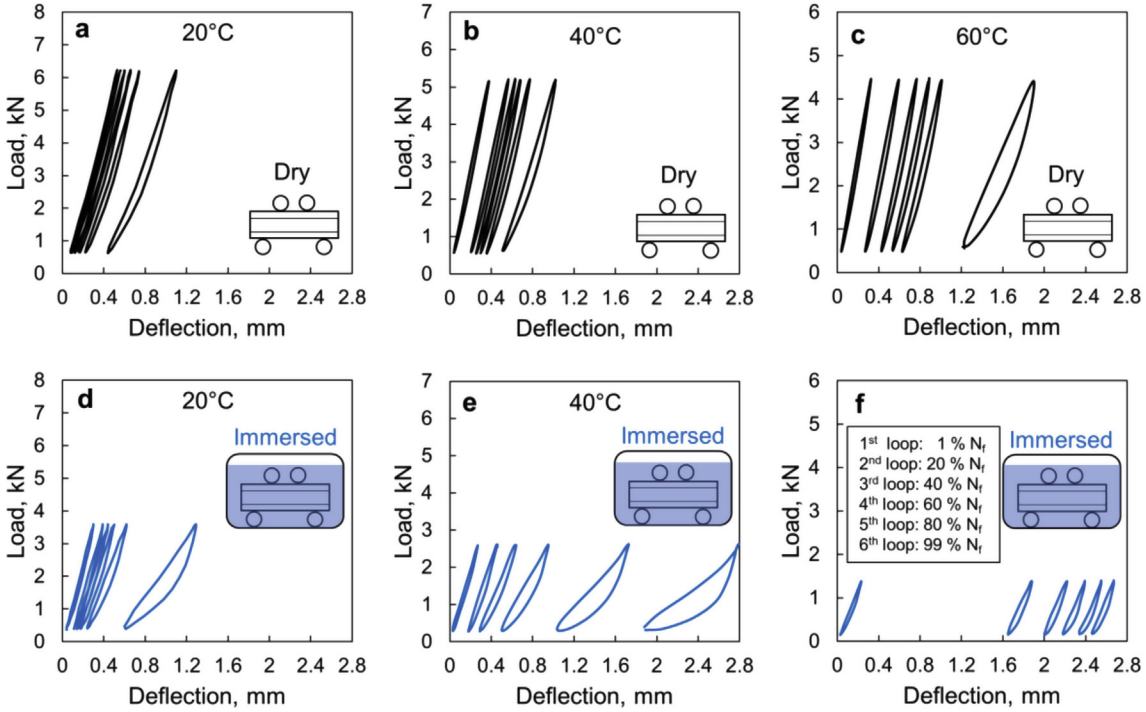

Fig. 8. Hysteresis loops at 1%, 20%, 40%, 60%, 80% and 99% of the fatigue life of dry and conditioned samples tested at (a, d) 20 °C, (b, e) 40 °C and (c, f) 60 °C.

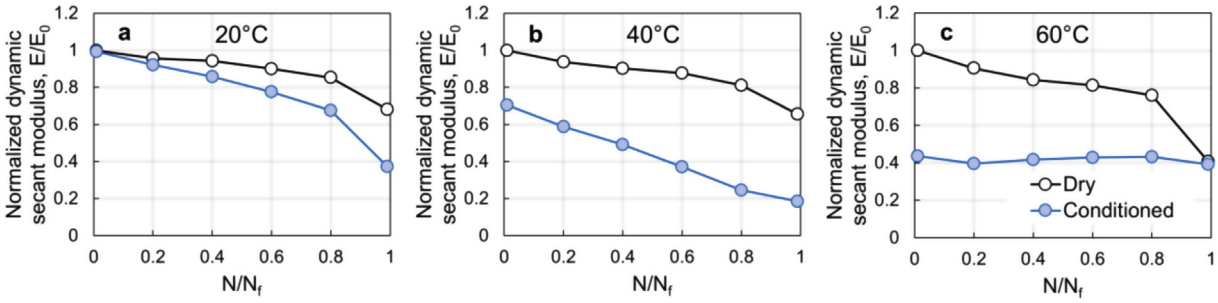

Fig. 9. Normalized dynamic secant modulus for dry and conditioned samples tested at (a) 20 °C, (b) 40 °C and (c) 60 °C.

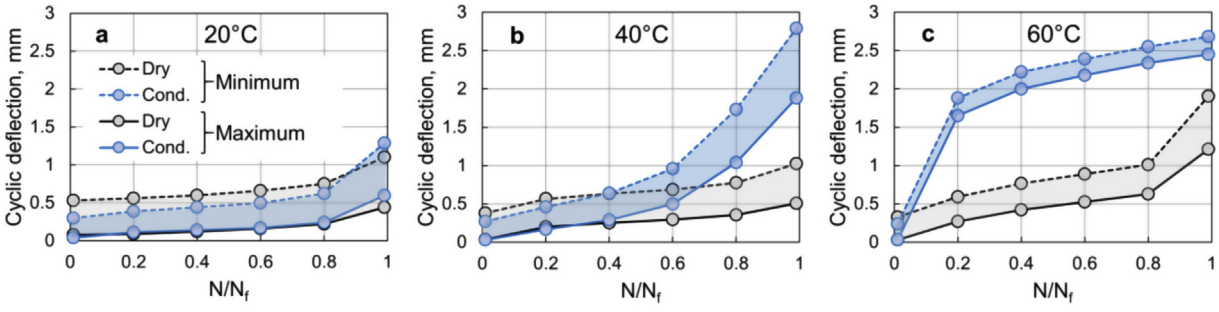

Fig. 10. Minimum and maximum cyclic deflection for dry and conditioned samples tested at (a) 20 °C, (b) 40 °C and (c) 60 °C.

found before loading the samples, which caused intra-ply cracks. This damage appears before testing, so it is independent on the temperature, hence the similar slope between 20 °C and 40 °C. The conditioned sample tested at 60 °C are above Tg, this explains the different slope observed for these samples.

The different failure mechanisms observed are reported for dry samples tested at room temperature, Fig. 15 (a), for the dry samples tested at higher temperatures, Fig. 15 (b) and for the conditioned samples tested in immersion, Fig. 15 (c).

4.3. Analytical modelling of the influence of temperature and moisture on fatigue

Several authors have worked on creep mastercurves for polymers and polymer reinforced composites [26–28]. Recent work from Nakada and Miyano has extended this approach for fatigue strength [19]. More recently, Motrazavian and Fatemi have employed this theory for building fatigue mastercurves of short fiber reinforced thermoplastics at different temperatures [18]. In the current work a model is developed for the construction of a fatigue mastercurve taking into account both

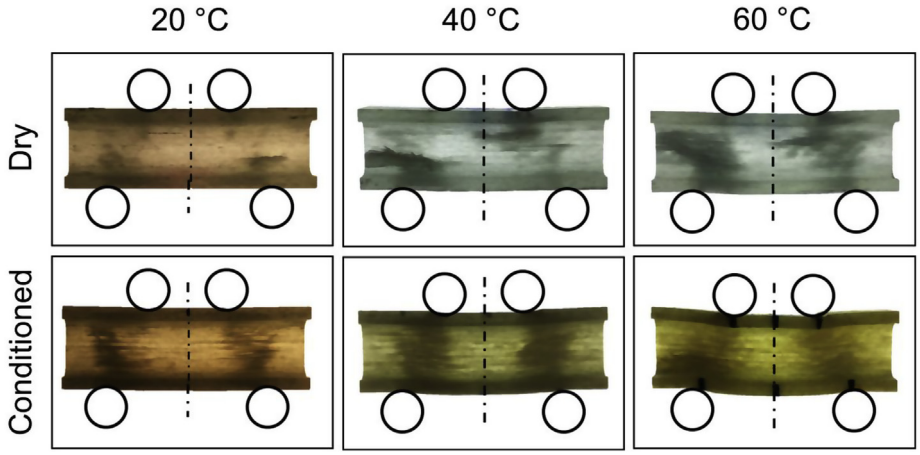

Fig. 11. Translucency pictures of tested samples.

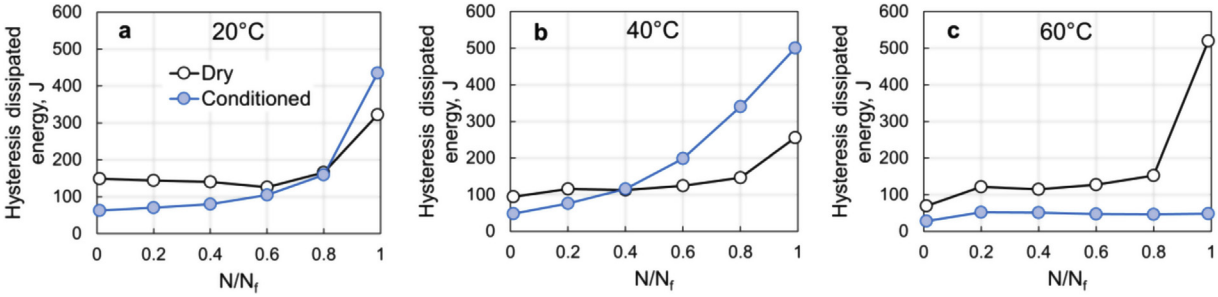

Fig. 12. Hysteresis dissipated energy for cycle for dry and conditioned samples tested at (a) 20 °C, (b) 40 °C and (c) 60 °C.

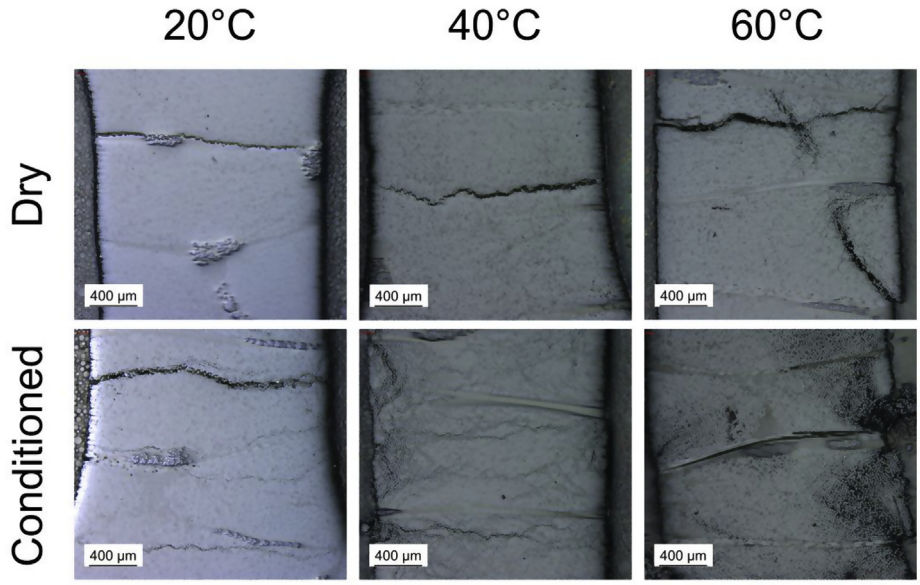

Fig. 13. An Optical micrograph of conditioned samples. Cracks develop inside the plies.

temperature and fluid saturation. The approach is based on the definition of an acceleration factor, or shift factor related to time:

$$\frac{t}{t_R} = a_t(T) \tag{2}$$

where t is the testing time under accelerated conditions, t_R is the testing time under reference conditions and a(T) is the acceleration factor or shift factor. When looking at fatigue the acceleration factor can be expressed in terms of number of cycles to failure:

$$\frac{N}{N_R} = a_N(T) \tag{3}$$

where N is number of cycles to failure under accelerated conditions, N_R is the number of cycles to failure as at a reference condition. Note that time and number of cycles to failure are related by the test frequency.

Interlaminar shear fatigue is a matrix dominated behaviour [14]. The increase of the mobility of molecular chain segments caused by an increase in temperature can accelerate the aging process of the polymer matrix. This acceleration can be described by an Arrhenius type

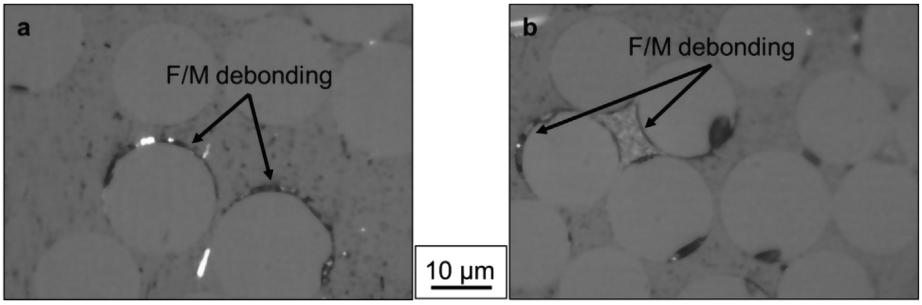

Fig. 14. An optical micrograph of conditioned samples prior to mechanical testing. Fiber/matrix debondings are visible inside the plies, (a) in areas where fibers are not closely packed and (b) in areas where fibers are closely packed.

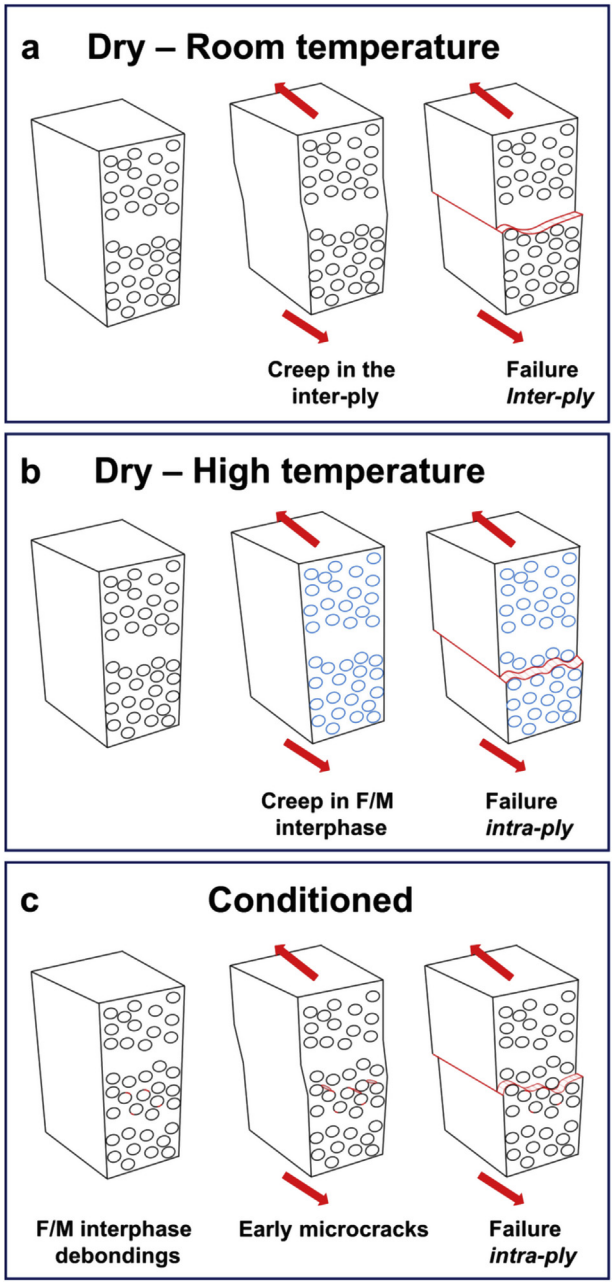

Fig. 15. Schematic explaining of the failure mechanism for (a) dry samples tested at room temperature, (b) dry samples tested at higher temperatures: 40 °C and 60 °C and (c) conditioned samples tested in immersion.

equation [29]:

$$t = t_R \exp\left(-\frac{\Delta H}{RT}\right) \tag{4}$$

where ΔH is the activation energy, R is the universal gas constant, T the absolute temperature and t_R is the testing time in reference conditions.

Fluid saturation causes a decrease of the glass transition temperature of the material. The decrease of the threshold between glassy state and rubbery state equivales to an increase of molecular chain mobility, even if the temperature of the specimen remains constant. It is therefore possible to define an equivalent temperature of the material, which takes into account the decrease of glass transition temperature:

$$T^* = T\,\frac{T_g^{dry}}{T_g^{cond}} \tag{5}$$

where T^* is the equivalent temperature, T is the absolute temperature, T_g^{dry} is the glass transition temperature of the dry material and T_g^{cond} is the glass transition temperature of the conditioned material.

The glass transition temperature of the material is influenced by the fluid content inside the material, assuming that the decrease of glass transition temperature is proportional to the moisture content, Eq. (5) can be written highlighting the fluid concentration link to the glass transition temperature:

$$T^* = T + T\left(\frac{T_g^{dry}}{T_g^{cond}(c)} - 1\right)\frac{c}{c_{eq}} \tag{6}$$

where c is the fluid concentration. Eq. (6) can therefore be written as:

$$t = t_r \exp\left(-\frac{\Delta H}{RT^*}\right) \tag{7}$$

Combining Eq. (2) and Eq. (7), it is possible to formulate the time-temperature shift factor as a function of temperature and fluid concentration:

$$\log a_t(T, c) = \log t - \log t_R = \frac{-\Delta A H}{2.303R}\left(\frac{1}{T_R} - \frac{1}{T^*}\right) \tag{8}$$

The activation energy is a material property that depends on the degradation mechanism, so for cases when different degradation mechanisms are expected the activation energy can change. The shift factor obtained in Eq. (8) refers to the testing time and in order to predict the number of cycles to failure this value needs to be multiplied for the test frequency.

$$\log a_N(T, c) = \log N - \log N_R = \frac{-\Delta H}{2.303R}\left(\frac{1}{T_R} - \frac{1}{T^*}\right) \tag{9}$$

In this theory the shift factor is calculated assuming that all tests are performed at the same frequency as the reference conditions. For tests performed at different frequencies, the theory would predict a frequency dependency of the results that has not been studied experimentally.

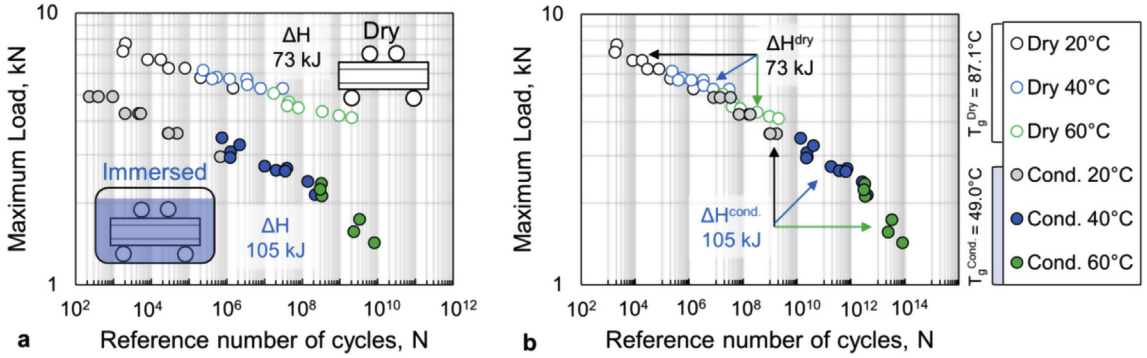

Fig. 16. (a) Dry and conditioned SN mastercurves (b) Environmental mastercurve with the definition of equivalent temperature. The glass transition temperature for each state is also indicated (dry and conditioned). The conditioned samples tested at 60 °C crosses the glass transition temperature of the material.

The dry and conditioned SN curves can be analysed separately in order to estimate the activation energy for each case, Fig. 16 (a). The values of the activation energy are 73 kJ for the dry samples and 105 kJ for the conditioned samples. Using the same values of activation energies and the definition of equivalent temperature introduced in Eq. (6) it is possible to build a time-temperature-environment mastercurve, Fig. 16 (b).

The mastercurves in Fig. 16 (a, b) are plotted in terms of reference number of cycles to failure, defined as time to failure in reference conditions, Eq. (7), multiplied by the test frequency. This definition enables differentiating the fatigue mastercurves from the fatigue curves obtained experimentally and shown in Fig. 7 [18].

The mastercurve obtained according to Eq. (9) provides a good fit with the experimental results in the range dry (20-40-60 °C) and conditioned (20–40 °C), Fig. 16 (b). The conditioned samples tested at 60 °C seem to deviate from the mastercurve and this effect is attributed to rubbery state of the material, which is tested above the glass transition temperature. In fact, the shift factor introduced in Eq. (9) is based on Arrhenius theory, which is not valid above the glass transition temperature of the material. The deviation of the conditioned samples tested at 60 °C from the linear mastercurve is an indication of the limits of validity of the mastercurve proposed here: the material should be below its glass transition temperature.

5. Conclusions

The combined effect of temperature and fluid immersion on the interlaminar shear fatigue strength of a glass fiber epoxy UD composite was studied. The micromechanical failure mechanism was investigated in each condition by analyzing the parameters of fatigue tests, leading to:

- matrix creep dominated failure for dry samples at 20 °C,
- fiber/matrix interface creep dominated failure for dry samples at higher temperatures (40 and 60 °C).
- failure dominated by cyclic growth of hygrothermal induced fiber/matrix debondings for the saturated samples tested at 20 and 40 °C,
- failure was due to rubbery state reached by the material, for the conditioned samples tested at 60 °C the, due to the drop of glass transition temperature below the testing temperature.

From these observations a novel Arrhenius based mastercurve was built for modelling the effect of temperature and fluid saturation, synthetizing six fatigue curves in a mastercurve. The glass transition temperature of the material, with its drop from dry to conditioned state, was proposed as a parameter enabling to represent both dry and saturated samples in the same mastercurve.

The model captures the different failure mechanism between dry and conditioned samples, as two different activation energies are obtained in these conditions, but a limitation remains the fact that the model is still phenomenological. A deeper understanding should enable to establish a link between the activation energy value and the failure mechanism observed. Another limitation is the fact that the model is proposed for a matrix dominated test mode, interlaminar shear. It should be studied the applicability of the model to other failure modes.

Declaration of interest

None.

Acknowledgements

This work is part of the DNV GL led Joint Industry Project “Affordable Composites” with nine industrial partners and the Norwegian University of Science and Technology (NTNU). The authors would like to express their thanks for the financial support by The Research Council of Norway (Project 245606/E30 in the Petromaks 2 programme).

The authors would like to thank also Carl-Magnus Midtbø, Børge Holen, Roar Munkebye and Emil Kulbotten for the design and realization of an immersed testing chamber.

References

[1] O.O. Ochoa, M.M. Salama, Offshore composites: transition barriers to an enabling technology, Compos. Sci. Technol. 65 (15–16) (2005) 2588–2596.
[2] M.M. Salama, et al., The first offshore field installation for a composite riser joint, 6–9 May, Offshore Technology Conference, 2002 Houston, Texas (USA), OTC-14018-MS.
[3] C. Baley, et al., Application of interlaminar tests to marine composites. A literature review, Appl. Compos. Mater. 11 (2) (2004) 99–126.
[4] ASTM, D2344/D2344M-16, Standard Test Method for Short-Beam Strength of Polymer Matrix Composite Materials and Their Laminates, ASTM International, West Conshohocken, PA, 2016.
[5] A.I. Gagani, E.P.V. Mialon, A.T. Echtermeyer, Immersed interlaminar fatigue of glass fiber epoxy composites using the I-beam method, Int. J. Fatigue 119 (2019) 302–310.
[6] A. Gagani, A. Krauklis, E. Sæter, N.-P. Vedvik, A.T. Echtermeyer, A Novel Method for Testing and Determining ILSS for Marine and Offshore Composites, (2019) Under Review.
[7] G. Springer, Environmental Effects on Composite Materials vol. 1, Technomic Publishing Company, 1984.
[8] G. Springer, Environmental Effects on Composite Materials vol. 2, CRC Press, 1984.
[9] C. Browning, G. Husman, J. Whitney, Moisture effects in epoxy matrix composites, in: J. Davis (Ed.), Composite Materials: Testing and Design (Fourth Conference), ASTM International, West Conshohocken, PA, 1977, pp. 481–496 1977.
[10] F.A. Ramirez, L.A. Carlsson, B.A. Acha, Evaluation of water degradation of vinylester and epoxy matrix composites by single fiber and composite tests, J. Mater. Sci. 43 (15) (2008) 5230–5242.
[11] S. Mallarino, J.F. Chailan, J.L. Vernet, Interphase investigation in glass fibre composites by micro-thermal analysis, Compos. Part A 36 (9) (2005) 1300–1306.
[12] Y. Joliff, L. Belec, J.F. Chailan, Modified water diffusion kinetics in an unidirectional glass/fibre composite due to the interphase area: experimental, analytical and numerical approach, Compos. Struct. 97 (2013) 296–303.
[13] Y. Joliff, et al., Study of the moisture/stress effects on glass fibre/epoxy composite and the impact of the interphase area, Compos. Struct. 108 (2014) 876–885.

[14] R.E. Lyon, D.L. Schumann, Determination of matrix-dominated mechanical properties of fiber composite lamina, Polym. Compos. 13 (1) (1992) 1–6.
[15] I.B.C.M. Rocha, et al., Hygrothermal ageing behaviour of a glass/epoxy composite used in wind turbine blades, Compos. Struct. 174 (Supplement C) (2017) 110–122.
[16] I.B.C.M. Rocha, et al., A combined experimental/numerical investigation on hygrothermal aging of fiber-reinforced composites, Eur. J. Mech. A Solid. 73 (2019) 407–419.
[17] J. Petermann, K. Schulte, The effects of creep and fatigue stress ratio on the long-term behaviour of angle-ply CFRP, Compos. Struct. 57 (1) (2002) 205–210.
[18] S. Mortazavian, A. Fatemi, Fatigue of short fiber thermoplastic composites: a review of recent experimental results and analysis, Int. J. Fatigue 102 (2017) 171–183.
[19] M. Nakada, Y. Miyano, Accelerated testing for long-term fatigue strength of various FRP laminates for marine use, Compos. Sci. Technol. 69 (6) (2009) 805–813.
[20] ASTM, Standard Test Method for Moisture Absorption Properties and Equilibrium Conditioning of Polymer Matrix Composite Materials, ASTM International, West Conshohocken, PA, 2014.
[21] A. Gagani, et al., Micromechanical modeling of anisotropic water diffusion in glass fiber epoxy reinforced composites, J. Compos. Mater. 52 (17) (2018) 2321–2335.
[22] S.P. Timoshenko, LXVI. On the correction for shear of the differential equation for transverse vibrations of prismatic bars, Lond. Edinb. Dublin. Phil. Mag. J. Sci. 41 (245) (1921) 744–746.
[23] O.H. Basquin, The exponential law of endurance tests, ASTM (Am. Soc. Test. Mater.)Proc. 10 (1910) 625-360.
[24] A. Manalo, et al., Temperature-sensitive mechanical properties of GFRP composites in longitudinal and transverse directions: a comparative study, Compos. Struct. 173 (2017) 255–267.
[25] P. Davies, M. Arhant, Fatigue behaviour of acrylic matrix composites: influence of seawater, Appl. Compos. Mater. (2018).
[26] H. Leaderman, Elastic and Creep Properties of Filamentous Materials, Massachusetts Institute of Technology, Cambridge, Mass, 1941.
[27] A.V. Tobolsky, R.D. Andrews, Systems manifesting superposed elastic and viscous behavior, J. Chem. Phys. 13 (1) (1945) 3–27.
[28] J. Honerkamp, J. Weese, A note on estimating mastercurves, Rheol. Acta 32 (1) (1993) 57–64.
[29] S. Arrhenius, Über die Dissociationswärme und den Einfluss der Temperatur auf den Dissociationsgrad der Elektrolyte, Z. Phys. Chem. (1889) 96.